Bridging the gap between Nonlinear Normal Modes and Modal Derivatives

Cees Sombroek, Ludovic Renson, Paolo Tiso, Gaetan Kerschen

Key words: Model Reduction, Nonlinear Normal Modes, Modal Derivatives, Quadratic Manifold Transformation

Abstract

Nonlinear Normal Modes (NNMs) have a clear conceptual relation to the classical linear normal modes (LNMs), yet they offer a solid theoretical framework for interpreting a wide class of non-linear dynamical phenomena with no linear counterpart. The main difficulty associated with NNMs is that their calculation for large-scale models is expensive, particularly for distributed nonlinearities. Repeated direct time integrations need to be carried out together with extensive sensitivity analysis to reproduce the frequency-energy dependence of the modes of interest.

In the present paper, NNMs are computed from a reduced model obtained using a quadratic transformation comprising LNMs and Modal Derivatives (MDs). Previous studies have shown that MDs can capture the essential dynamics of geometrically nonlinear structures and can greatly reduce the computational cost of time integration.

A direct comparison with the NNMs computed from another standard reduction technique highlights the capability of the proposed reduction method to capture the essential nonlinear phenomena. The methodology is demonstrated using simple examples with 2 and 4 degrees of freedom.

1 Introduction

The manifestation of nonlinear phenomena during the vibration testing of aerospace structures is frequently reported in the technical literature (e.g., for the Airbus A400M [1] and for the F-16 aircraft [2]). A common source of nonlinearity is the junction between structural components where freeplay and complex damping

mechanisms can be present. The stringent constraints on weight also lead to more flexible structures where geometrical nonlinear effects are present due to large displacements and rotations.

Though frequently ignored in practice, the presence of nonlinearity poses important challenges as novel dynamical phenomena with no linear counterpart may be observed. Modal interactions, for instance, couple the vibration modes of a structure and can lead to energy transfers that can in turn jeopardize the structural integrity (cf. [3]). Addressing nonlinearity as early as in the design becomes therefore important.

In this context, the concept of nonlinear normal modes (NNMs) proved useful. First introduced in the 1960s by Rosenberg, NNMs were defined as families of synchronous periodic oscillations [4, 5]. An extended definition considering NNMs as *(non-necessarily synchronous) periodic motions* was then proposed in [6] to account for modal interactions during which the periodic motion contains the frequencies of at least two interacting modes. Considered as the direct extension of linear vibration modes (VMs) to nonlinear systems, NNMs allow to rigorously interpret nonlinear dynamical phenomena such as mode localization, internal resonances and mode bifurcations [7].

With the advances in computing power and in computer methods, recent years witnessed the development of computational methods for NNMs. In Ref. [8], shooting and pseudo-arclength continuation methods are combined to calculate NNMs. Alternatively, the harmonic balance and asymptotic numerical methods are used in Ref. [9]. The main difficulty associated with NNMs is that their calculation for large-scale models is expensive. If the aforementioned techniques were applied to real-life structures [10, 3], the systems mainly consisted in large linear structures with localized nonlinearities. In this case, classical linear reduction methods, such as the Craig-Bampton or the Rubin techniques, can be used to accurately and effectively reduce the dimensionality of the linear system. However, for systems with nonlinear geometrical effects, nonlinearities are distributed between all DOFs and such linear approach proved ineffective.

In previous contributions [11, 12, 13], an effective model reduction of geometrically nonlinear problems was achieved by combining VMs and modal derivatives (MDs) in a single basis. Time simulations showed that the essential dynamics of the structures was captured while computational efforts were effectively reduced. Simple, this approach has however the drawback of largely increasing the size of the reduced-order model as the number of MDs grows quadratically with the number of degrees of freedom (DOF).

In this paper, we present and investigate an alternative approach where VMs and MDs are combined in a quadratic coordinate transformation. The proposed method fully exploits the second-order Taylor-series expansion of the displacement vector with respect to a reduced set of vibration modes. This differs from previous works where a linear basis with additional coordinates for each MDs was built.

The paper is organized as follows. Section 2 introduces the governing equations of motion and Section 3 presents the underlying theory behind classical Galerkin model reduction techniques and introduces the concept of modal derivatives. In

Section 4, the new quadratic transformation is derived. The method used for computing NNMs is briefly introduced in Section 5. The quadratic manifold approach is exploited in Section 6 using examples with 2 and 4 DOFs. A direct comparison with the NNMs computed from the full system and from systems reduced with the Galerkin method are used to discuss the performance of the proposed method.

2 Governing Equations

We seek the solution of the space discretized equation of motion of a generic system:

$$\begin{cases} \mathbf{M}\ddot{\mathbf{y}}(t) + \mathbf{K}\mathbf{y}(t) + \mathbf{f}^{nl}(\mathbf{y}(t)) = \mathbf{p}(t) \\ \mathbf{y}(0) = \mathbf{y}_0 \\ \dot{\mathbf{y}}(0) = \dot{\mathbf{y}}_0, \end{cases} \tag{1}$$

where $\mathbf{y}(t) \in \mathbb{R}^n$ s the generalized displacement vector, $\mathbf{M} \in \mathbb{R}^{n\times n}$ and $\mathbf{K} \in \mathbb{R}^{n\times n}$ are the mass and linear stiffness matrices, respectively, $\mathbf{f}^{nl}(\mathbf{y}(t)) : \mathbb{R}^n \mapsto \mathbb{R}^n$ is the nonlinear force vector and $\mathbf{p}(t) \in \mathbb{R}^n$ is the time dependent applied load vector. Note that we explicitly separate the linear and the nonlinear internal forces. The initial conditions for the displacement and the velocity vector are indicated with $\mathbf{y}_0$ and $\dot{\mathbf{y}}_0$, respectively. From this point on, the time dependency is omitted for clarity.

3 Galerkin Projection

In practical applications, the size n of Eq. (1) is usually large. The number of unknowns can be reduced to k, with $k \ll n$, by projecting the displacement field $\mathbf{y}$ on a suitable reduced order basis (ROB) $\Psi \in \mathbb{R}^{n\times k}$ of time-independent vectors, as:

$$\mathbf{y} \approx \Psi\mathbf{q}, \tag{2}$$

where $\mathbf{q}(t) \in \mathbb{R}^k$ is the vector of modal amplitudes. The governing equations can then be projected on the chosen basis Ψ in order to make the equilibrium residual orthogonal to the subspace in which the solution $\mathbf{q}$ is sought. This results in a reduced system of k nonlinear equations:

$$\Psi^T\mathbf{M}\Psi\ddot{\mathbf{q}}(t) + \Psi^T\mathbf{K}\Psi\mathbf{q} + \Psi^T\mathbf{f}^{nl}(\Psi\mathbf{q}) = \Psi^T\mathbf{p}, \tag{3}$$

or, equivalently,

$$\hat{\mathbf{M}}\ddot{\mathbf{q}} + \hat{\mathbf{K}}\mathbf{q} + \hat{\mathbf{f}}^{nl}(\Phi\mathbf{q}) = \hat{\mathbf{p}}. \tag{4}$$

The reduced mass matrix $\hat{\mathbf{M}}$ and stiffness matrix $\hat{\mathbf{K}}$ do not depend on $\mathbf{q}$ and can be calculated offline. We refer to the numerical solution $\mathbf{y}$ of Eq. (1) as the *full* solution, while $\mathbf{u} = \Psi\tilde{\mathbf{q}}$ is called *reduced* solution, $\tilde{\mathbf{q}}$ being the solution of Eq. (4). The key of

a good reduction method is to find a suitable ROB Ψ that is able to reproduce the full solution with a good, hopefully controlled, accuracy. Note here that Galerkin projection is not strictly the only possible choice, since also the Petrov-Galerkin method can be applied. In this method, the ROB for the left projection is different than the ROB for the primary variable. Usually, the Galerkin method is preferred in structural dynamics applications because of the symmetry and positive definiteness of the tangential operators.

3.1 Vibration modes

Let us consider a static equilibrium position $\mathbf{y}_{eq}$ when the applied load is constant and given by $\mathbf{p}_{eq}$. We can then linearize the system of equations (1) around such configuration assuming that the motion $\mathbf{u}$ around $\mathbf{y}_{eq}$ is small, i.e. $\mathbf{y} = \mathbf{y}_{eq} + \mathbf{u}$, $\ddot{\mathbf{y}} = \ddot{\mathbf{u}}$. The linearized dynamic equilibrium equations become:

$$\mathbf{M}\ddot{\mathbf{u}} + \mathbf{K}\mathbf{u} = \mathbf{s} \tag{5}$$

where $\mathbf{s}$ is a small load variation from $\mathbf{p}_{eq}$. The eigenvalue problem associated to equation (5) writes:

$$\left(\mathbf{K} - \omega_i^2 \mathbf{M}\right) \phi_i = \mathbf{0}, \;\; i = 1, 2, \ldots, N \tag{6}$$

and its solution provides n vibration modes (VMs) ϕ_i and associated natural frequencies ω_i^2. In linear modal analysis, the displacement vector $\mathbf{u}$ can be expressed as a linear combination of $m < n$ VMs as:

$$\mathbf{u} = \sum_{i=1}^{m} \phi_i(\mathbf{y}_{eq}) q_i = \Phi \mathbf{q} \tag{7}$$

where $\Phi = [\phi_1 \ldots, \phi_m] \in \mathbb{R}^{n \times m}$. In linear analysis, the VMs ϕ_i are costant, i.e. they form a ROB that spans the small motion $\mathbf{u}$ around $\mathbf{y}_{eq}$. We discuss the implication of large displacements on the ROB in the next section.

3.2 Modal Derivatives

The projection of the governing equations on a reduction basis formed by a reduced set of VMs is a well-known technique for linear structural dynamics. The main advantage of this technique is that the resulting reduced model consists of a system of uncoupled equations that can therefore be solved separately. As discussed in the introduction, several attempts has been made to extend the vibration modes projection for nonlinear analysis. The main limitation of such approach lies in the fact that the vibration basis changes as the configuration of the system changes. It is therefore

required to upgrade the basis during the numerical time integration to account for the effect of the nonlinearity.

When the displacements can not be considered as small, the VMs change with respect to the configuration. We can therefore express the displacement vector $\mathbf{u}$ as

$$\mathbf{u} = \sum_{i=1}^{M} \phi_i(\mathbf{y}_{eq} + \mathbf{u}) q_i \tag{8}$$

where the dependence of the VMs on the displacement is highlighted. If Eq. (8) is expanded in Taylor series around the equilibrium configuration $\mathbf{y}_{eq}$:

$$\mathbf{u} = \sum_{i=1}^{M} \phi_i(\mathbf{y}) q_i = \frac{\partial \mathbf{u}}{\partial q_i}\Big|_{\mathbf{u}=\mathbf{0}} q_i + \frac{1}{2} \frac{\partial^2 \mathbf{u}}{\partial q_i \partial q_j}\Big|_{\mathbf{u}=\mathbf{0}} q_i q_j + \dots \tag{9}$$

The derivatives of the displacement vector with respect to the modal amplitudes q_i can be computed from equation (8), and are:

$$\frac{\partial \mathbf{u}}{\partial q_i} = \phi_i + \frac{\partial \phi_j}{\partial q_i} q_j \tag{10}$$

and

$$\frac{\partial^2 \mathbf{u}}{\partial q_i \partial q_j} = \frac{\partial \phi_i}{\partial q_j} + \frac{\partial \phi_j}{\partial q_i} + \frac{\partial^2 \phi_k}{\partial q_i \partial q_j} q_k \tag{11}$$

.

When evaluated at $\mathbf{y} = \mathbf{y}_{eq}$, they become:

$$\frac{\partial \mathbf{u}}{\partial q_i}\Big|_{\mathbf{u}=\mathbf{0}} = \phi_i \tag{12}$$

and

$$\frac{\partial^2 \mathbf{u}}{\partial q_i \partial q_j}\Big|_{\mathbf{u}=\mathbf{0}} = \frac{\partial \phi_i}{\partial q_j} + \frac{\partial \phi_j}{\partial q_i} \tag{13}$$

The term (12) is the VM, while $\frac{\partial \phi_i}{\partial q_j}$ is the MD: it represents how the VM ϕ_i changes when the system is perturbed in the shape of VM ϕ_i.

A way to compute $\frac{\partial \phi_i}{\partial q_j}$ is to differentiate the eigenvalue problem (6) with respect to the modal amplitudes:

$$\left[\mathbf{K}_{eq} - \omega_i^2 \mathbf{M}\right] \frac{\partial \Phi_i}{\partial q_j} + \left[\frac{\partial \mathbf{K}_{eq}}{\partial q_j} - \frac{\partial \omega_i^2}{\partial q_j}\mathbf{M}\right] \Phi_i = \mathbf{0}, \tag{14}$$

together with orthogonality condition

$$\Phi_i^T \mathbf{M} \frac{\partial \Phi_j}{\partial q_k} = \mathbf{0}, \;\; \forall, i, j, k = 1, \dots, m, \tag{15}$$

that must be added to in order to 14 to make the expansion 9 unique. Essentially, Eq. (14) yields the sensitivity of the VMs with respect to the modal amplitudes. In previous contributions [11, 12, 13], it has been shown that an effective ROB for

geometrically nonlinear problems of the type governed by Eq. (1) can be formed by combining dominant VMs with some MDs, as:

$$\Psi = [\Phi_1, \ldots, \Phi_m, \ldots, \frac{\partial \Phi_i}{\partial q_j}, \ldots], \tag{16}$$

While simple and effective, this approach bears the drawback of largely increasing the size of the ROB, as the number of MDs grows quadratically with m. We present in Section 4 an alternative approach that fully exploits the structure of Eq. (9).

4 Reduction with quadratic manifold

The expansion (9) essentially provides a quadratic mapping $\mathbf{U}(\mathbf{q}) : \mathbb{R}^m \mapsto \mathbb{R}^n$ between the modal coordinates $\mathbf{q}$ and the physical displacements $\mathbf{u}$. Compactly, we can write:

$$\mathbf{u} = \mathbf{U}(\mathbf{q}) = \Phi\mathbf{q} + \frac{1}{2}\Theta(\mathbf{q}, \mathbf{q}) \tag{17}$$

where the third order tensor $\Theta \in \mathbb{R}^{n\times n\times n}$ writes componentwise:

$$\Theta_{Iij} = \frac{\partial \phi_i}{\partial q_j} + \frac{\partial \phi_j}{\partial q_i} \tag{18}$$

and $\Theta_{Iij} = \Theta_{Iji}$

The velocity and acceleration are then expressed as functions of the modal coordinates q_I as

$$\dot{\mathbf{u}} = \Phi\dot{\mathbf{q}} + \Theta(\dot{\mathbf{q}}, \mathbf{q}) \tag{19}$$

and

$$\ddot{\mathbf{u}} = \Phi\ddot{\mathbf{q}} + \Theta(\ddot{\mathbf{q}}, \mathbf{q}) + \Theta(\dot{\mathbf{q}}, \dot{\mathbf{q}}), \tag{20}$$

respectively. The tangent space $\mathbf{V}(\mathbf{q}) \in \mathbb{R}^{n\times m}$ is computed as:

$$\mathbf{V} = \frac{\partial \mathbf{U}}{\partial \mathbf{q}} = \Phi + \Theta(\mathbf{q}, \cdot) \tag{21}$$

The notation $\Theta(\mathbf{q}, \cdot)$ is to be intended, componentwise, as $\Theta_{Iij}q_i = \Theta_{Iij}q_j$. When inserting the quadratic manifold approximation (17) in the governing equation (1) and projecting on the tangent subspace (21) we obtain the reduced governing equations:

$$\ddot{\mathbf{q}} + \mathbf{M}_3(\mathbf{q}, \ddot{\mathbf{q}}, \mathbf{q}) + \mathbf{M}_3(\mathbf{q}, \dot{\mathbf{q}}, \dot{\mathbf{q}}) + \mathbf{V}^T\mathbf{f}^{int}(\mathbf{U}(\mathbf{q})) = \mathbf{V}^T\mathbf{p} \tag{22}$$

where $\mathbf{M}_{3Iijk} = \Theta_{iIJ}\mathbf{M}_{ij}\Theta_{jKL}$ and orthogonality and mass-normalization has been employed. As compared to the Galerkin projected equations 4 when VMs and MDs are used to form the ROB, the reduced system 22 is much more compact (size m as

compared to size $m+m^2$). This approach is analogous to [14], where the nonlinear manifold is constructed via a static condensation procedure.

5 Nonlinear Normal Modes

In the conservative case, NNMs can be sought numerically as periodic solutions of the governing nonlinear equations of motion, i.e., Eqs. (1,4,22) for the full system, the system reduced using a Galerkin-type projection, and the QM approach, respectively. To this end, the two-step algorithm presented in Ref. [8] is exploited in the present study. This section provides a succinct description of the shooting and pseudo-arclength techniques used in the algorithm.

Shooting is a popular numerical technique for solving the two-point boundary-value problem associated with the periodicity condition

$$\mathbf{H}(T,\mathbf{z}_{p_0}) = \mathbf{z}_p(T,\mathbf{z}_{p_0}) - \mathbf{z}_{p_0} = \mathbf{0} \tag{23}$$

where $\mathbf{H}(T,\mathbf{z}_{p_0})$ is called the shooting function, and $\mathbf{z}$ is the state vector of the system. $\mathbf{H}$ expresses the difference between the final state at time T of the system $\mathbf{z}_p(T,\mathbf{z}_{p_0})$ and the initial state of the system $\mathbf{z}_{p_0}$. A solution $\mathbf{z}_p(t,\mathbf{z}_{p_0})$ is periodic if $\mathbf{z}_p(t,\mathbf{z}_{p_0}) = \mathbf{z}_p(t+T,\mathbf{z}_{p_0})$ where T is the minimal period. In a shooting algorithm, the period T and the initial conditions $\mathbf{z}_{p_0}$ realizing a periodic motion are found iteratively. More specifically, direct numerical integration is carried out to obtain an initial guess of the periodic solution, which is corrected by means of a Newton-Raphson procedure to converge to the actual solution. In this work, time integration is performed using a fifth-order Runge-Kutta scheme with an automatic selection of the time step.

Another important remark in the resolution of the boundary-value problem formulated in Eq. (23) is that the phase of the periodic solutions is not unique. If $\mathbf{z}_p(t)$ is solution of the equations of motion, then $\mathbf{z}_p(t+\Delta t)$ is geometrically the same solution in state space for any Δt. Hence, an additional condition $h(\mathbf{z}_{p_0}) = 0$, termed phase condition, is specified to remove the arbitrariness of the initial conditions. Following the approach in Ref. [8], the modal velocities are set equal to zero. In summary, an isolated NNM motion is computed by solving the augmented two-point boundary-value problem defined by the two relations

$$\mathbf{H}(T,\mathbf{z}_{p_0}) = \mathbf{0}, \tag{24}$$

$$h(\mathbf{z}_{p_0}) = 0. \tag{25}$$

To obtain the family of periodic solutions that describe the considered NNM, shooting is combined with a pseudo-arclength continuation technique. Starting from a known periodic solution, continuation proceeds in two steps, namely a prediction and a correction, as illustrated in Fig. 1. In the prediction step, a guess of the next periodic solution along the NNM branch is generated in the direction of the tangent

vector to the branch at the current solution. Next, the prediction is corrected using a shooting procedure, forcing the variations of the period and the initial conditions to be orthogonal to the prediction direction.

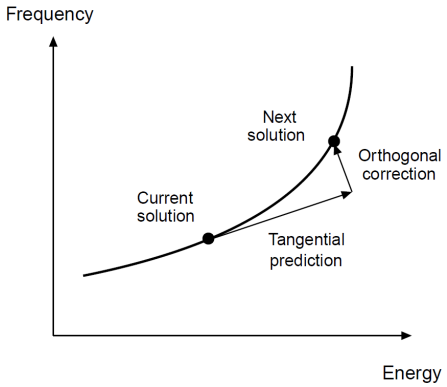

Fig. 1 Schematic representation of the prediction and correction steps of the pseudo-arclength continuation scheme.

6 Numerical Examples

We intend here to present simple tests to compare the exact NNMs obtained via continuation method to the NNMs calculated with the MDs based reduced order models (4) and (22). This is done using two examples containing 2 DOFs and 4 DOFs respectively.

6.1 2DOF Example

First a two DOFs system is examined with geometrical nonlinearities (quadratic and cubic) arising from second order terms in the strain tensor. The configuration of the system is shown in Figure(2). The equations of motion for the system write:

$$\begin{cases} m\ddot{x}_1 + k_1 x_1 + k_2 x_1 x_2 + \frac{3k_1 x_1^2}{2} + \frac{k_1 x_2^2}{2} + \frac{(k_1+k_2)x_1}{2}\left(x_1^2+x_2^2\right) = 0 \\ m\ddot{x}_2 + k_2 x_2 + k_1 x_1 x_2 + \frac{3k_2 x_2^2}{2} + \frac{k_2 x_1^2}{2} + \frac{(k_1+k_2)x_2}{2}\left(x_1^2+x_2^2\right) = 0 \end{cases} \tag{26}$$

where the parameters are set to be $k_1 = k_2 = 1\ N/m$ and $m = 1\ kg$ such that the eigenfrequencies of the system become $\omega_1 = 1\ rad/s$ and $\omega_2 = \sqrt{3}\ rad/s$.

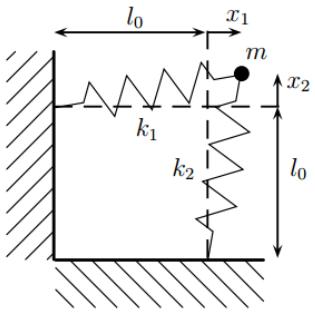

Fig. 2 Schematic representation of the 2 DOF system

To validate the proposed quadratic manifold formulation, the NNMs are computed in physical space, and with the proposed quadratic manifold Eq.(17) with two modal coordinates, so no reduction. NNM1 and NMM2 are presented in Figures (3, 4) using a frequency energy plot (FEP) (as suggested by [8]). From these figures, it is confirmed that considering two modes provides a full system transformation that results in the same exact FEP.

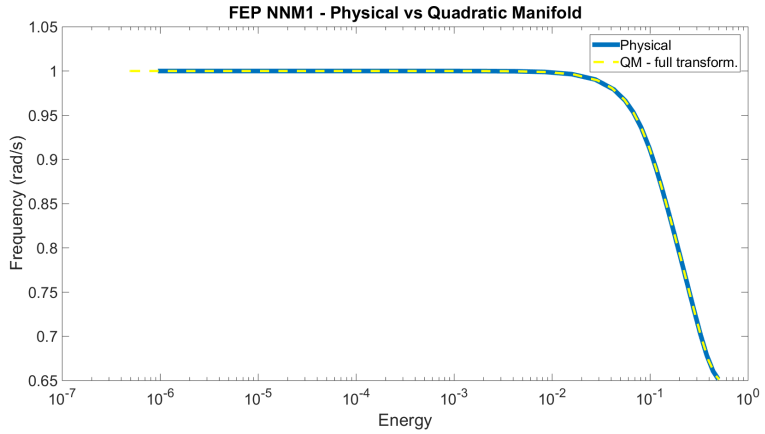

Fig. 3 FEP of first nonlinear normal mode

Next the reduction methods are used to compute NNM motion in a reduced sense. For the Galerkin projection two ROB are formed containing $[\phi_i]$ and $\left[\phi_i, \frac{\partial \phi_i}{\partial q_j}\right]$ respectively. Note that in the latter situation the system is actually not reduced, and therefore must produce the exact NNM. The quadratic manifold computation was carried out with a single modal coordinate q.
From the FEPs, shown in Figure(5) and Figure(6), it is clear that the Galerkin projection with the modal derivative enhanced ROB produces the exact NNM. Regarding

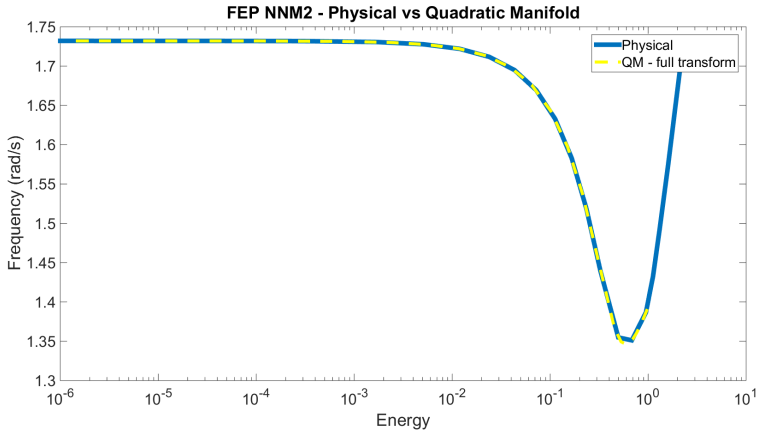

Fig. 4 FEP of second nonlinear normal mode

the results with actual reduction, the QM captures correctly the global trend of the FEP whereas the GP is qualitatively correct for the second NNM and wrong for the first one. One can also note that, for the first NNM, the branch computed with the QM deviates earlier from the true solution than the branch obtained with GP.

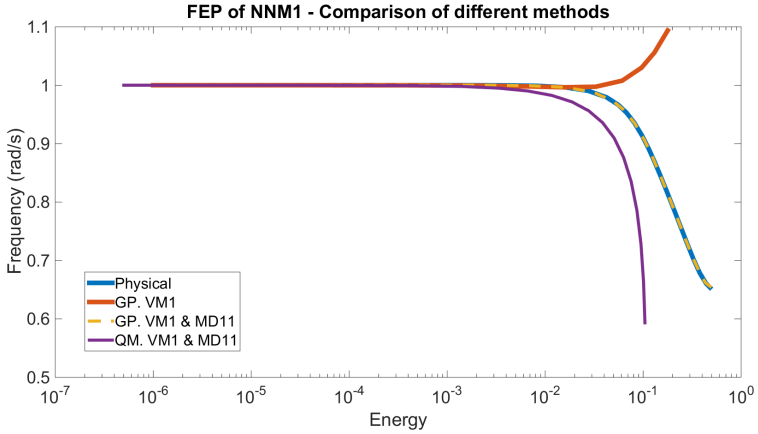

Fig. 5 Comparison of the reduction methods in the FEP of NNM1

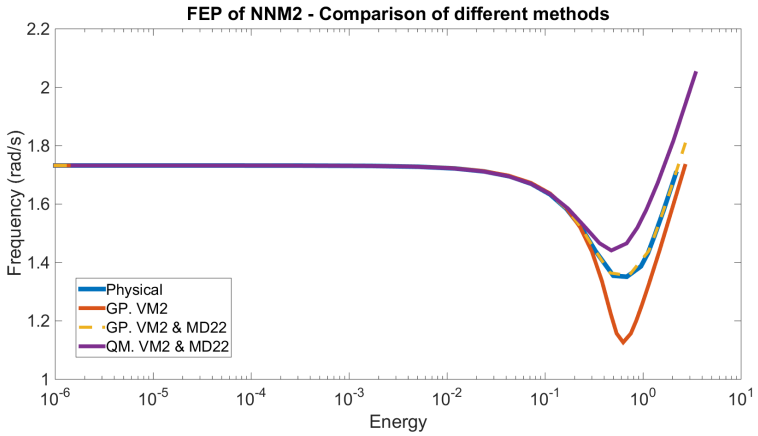

Fig. 6 Comparison of the reduction methods in the FEP of NNM2

6.2 4DOF Example

The second example contains 4 DOF, and the nonlinearities are again of geometrical nature. The configuration is presented in Figure(7). The equations of motions are given by:

$$\begin{cases} m_1\ddot{x_1} - \frac{k_2(l_0-x_1+x_2)\left((y_1-y_2)^2+(l_0-x_1+x_2)^2-L_0^2\right)}{2L_0^2} + \frac{k_1(l_0+x_1)\left((l_0+x_1)^2-L_0^2+y_1^2\right)}{2L_0^2} = 0 \\ m_1\ddot{y_1} + \frac{k_1y_1\left((l_0+x_1)^2-L_0^2+y_1^2\right)}{2L_0^2} + \frac{k_2(y_1-y_2)\left((y_1-y_2)^2+(l_0-x_1+x_2)^2-L_0^2\right)}{2L_0^2} = 0 \\ m_2\ddot{y_1} - \frac{k_3(l_0-x_2)\left((l_0-x_2)^2-L_0^2+y_2^2\right)}{2L_0^2} + \frac{k_2(l_0-x_1+x_2)\left((y_1-y_2)^2+(l_0-x_1+x_2)^2-L_0^2\right)}{2L_0^2} = 0 \\ m_2\ddot{y_2} - \frac{k_2(y_1-y_2)\left((y_1-y_2)^2+(l_0-x_1+x_2)^2-L_0^2\right)}{2L_0^2} + \frac{k_3y_2\left((l_0-x_2)^2-L_0^2+y_2^2\right)}{2L_0^2} = 0 \end{cases} \tag{27}$$

where the parameters are set to be $k_1 = k_2 = k_3 = 1\ N/m$, $m_1 = m_2 = 1\ kg$ and the original lengths of the springs are $L_0 = 0.4\ m$. A pretension is applied by suspending the masses at a distance $l_0 = 0.5\ m$ from the hinges and each other. The pretension is applied to separate the eigenfrequencies of the in plane and out of plane motion, these frequencies are $\omega_1 = 0.53\ rad/s$, $\omega_2 = 0.92\ rad/s$, $\omega_3 = 1.36\ rad/s$ and $\omega_4 = 2.35\ rad/s$.

The first nonlinear normal modes obtained with the full system and both reduction methods is presented in Figure(8) accompanied by a close up for very small energy (Figure 9). The results in both figures indicate that the QM is less accurate compared to a classical GP. However, if we look at the results in a frequency-amplitude plot (see Figures (10) and (11)), the QM is able to approximate the motion in both in and out of plane motion up to approximately 30% of the suspended spring lengths,

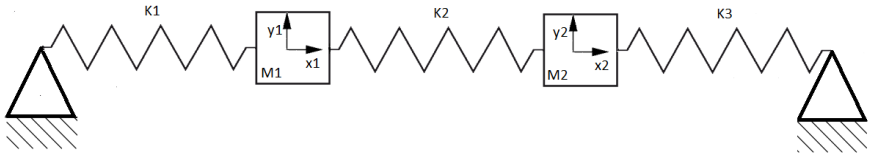

Fig. 7 Schematic representation of the 4 DOF system

whilst the GP can only approximate the result in one direction (not not along x_1). From this point of view, the QM improved the results with respect to a simple GP.

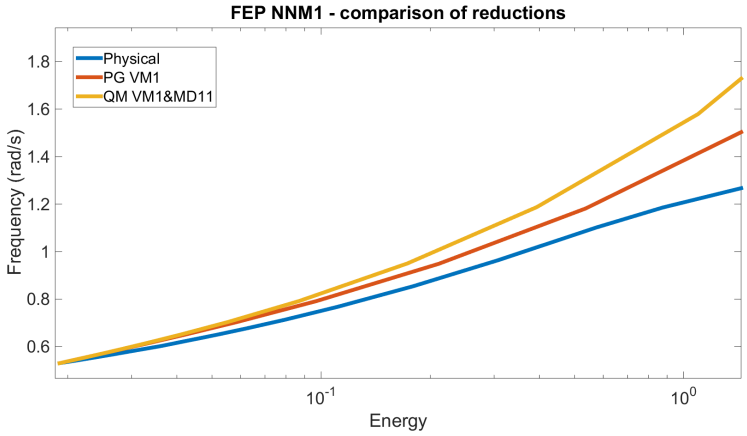

Fig. 8 NNM1 FEP, reduction methods compared with exact physical NNM

The results for the second NNM are presented in Figures (12, 13) and confirm our initial observations. More precisely, the QM is here more accurate than the GP throughout the energy range considered.

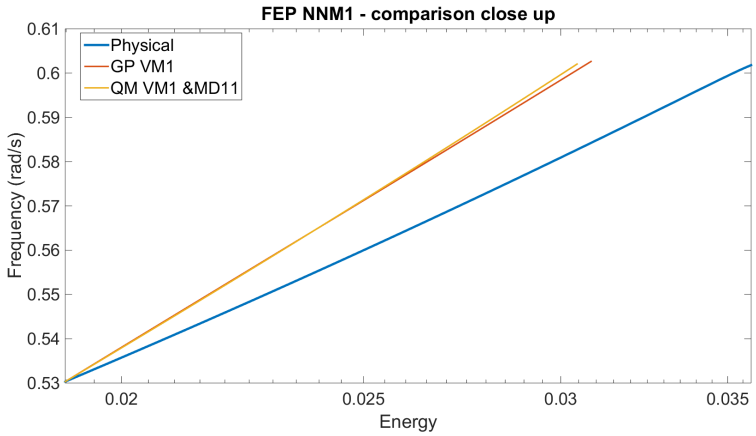

Fig. 9 Close up of NNM1 FEP, reduction methods compared with exact physical NNM

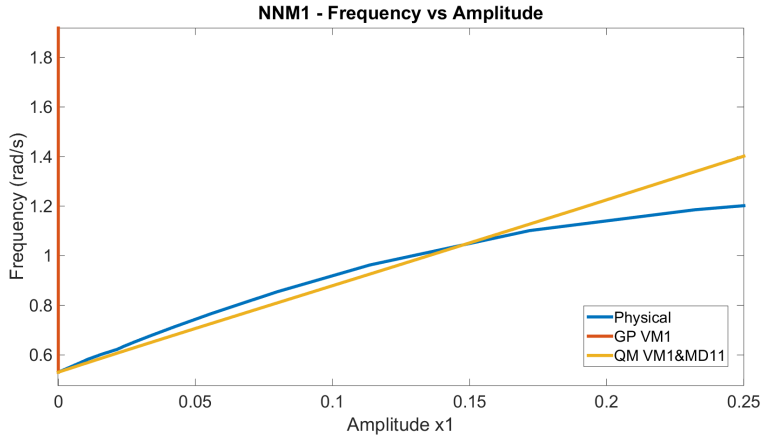

Fig. 10 NNM1 Frequency amplitude plot for x_1

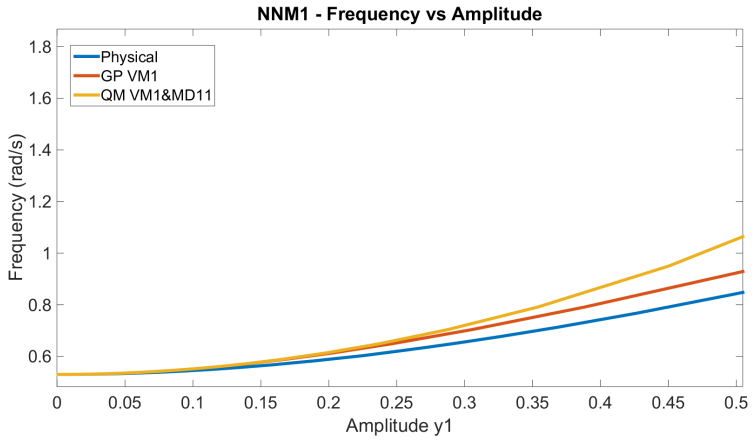

Fig. 11 NNM1 Frequency amplitude plot for y_1

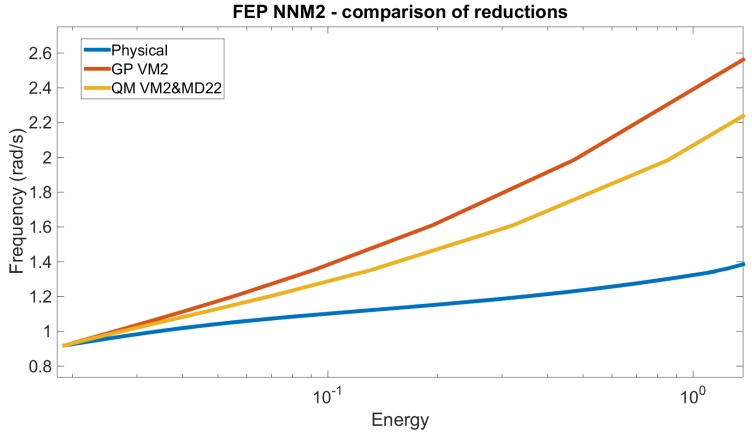

Fig. 12 NNM2 FEP, reduction methods compared with exact physical NNM

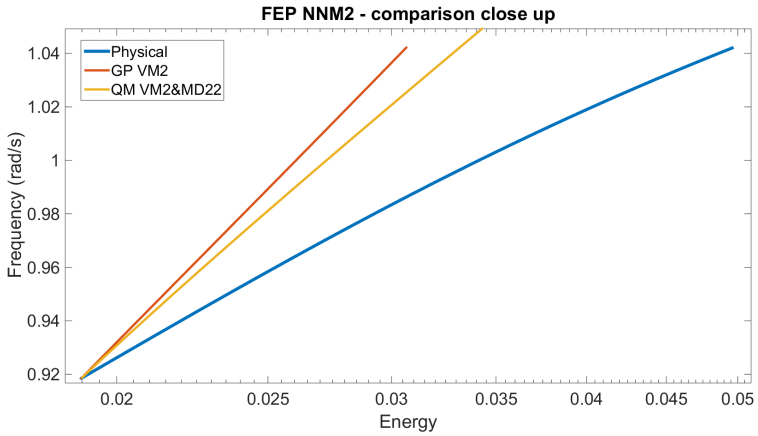

Fig. 13 Close up of NNM2 FEP, reduction methods compared with exact physical NNM

7 Conclusions

In this paper, a quadratic coordinate transformation combining linear VMs and their corresponding MDs was presented. In comparison with classical Galerkin reduction methods where each MD is associated with an independent DOF in the reduced system, the proposed method allows to further reduce the size of the dynamical system while accounting for the change of the VMs due to nonlinearities. The QM reduction was applied to two examples with 2 and 4 DOFs, respectively. For reduced-order models of same dimensions, the QM reduction showed to improve the results obtained with the simple Galerkin projection.

We however stress that the presented results are only preliminary and further investigations should be conducted. In particular, the improvements brought by the QM were only present for very low energies (or amplitudes).

References

1. J. R. Ahlquist, J. M. Carreño, H. Climent, R. de Diego, and J. de Alba. Assessment of nonlinear structural response in A400M GVT. In *Proceedings of the International Modal Analysis Conference, Jacksonville, FL, USA*, 2010.
2. J. P. Noël, L. Renson, G. Kerschen, B. Peeters, S. Manzato, and J. Debille. Nonlinear dynamic analysis of an F-16 aircraft using GVT data. In *Proceedings of the International Forum on Aeroelasticity and Structural Dynamics, Bristol, UK*, 2013.
3. L. Renson, J. P. Noël, and G. Kerschen. Complex dynamics of a nonlinear aerospace structure: numerical continuation and normal modes. *Nonlinear Dynamics, DOI 10.1007/s11071-014-1743-0*.
4. R. M. Rosenberg. Normal modes of nonlinear dual-mode systems. *Journal of Applied Mechanics*, 27(2):263–268, 1960.
5. R. M. Rosenberg. On nonlinear vibrations of systems with many degrees of freedom. *Advances in Applied Mechanics*, 9:155–242, 1966.
6. Y. S. Lee, G. Kerschen, A. F. Vakakis, P. Panagopoulos, L. Bergman, and D. M. McFarland. Complicated dynamics of a linear oscillator with a light, essentially nonlinear attachment. *Physica D: Nonlinear Phenomena*, 204(1-2):41–69, 2005.
7. A. F. Vakakis, L. I. Manevitch, Y. V. Mlkhlin, V. N. Pilipchuk, and A. A. Zevin. *Normal Modes and Localization in Nonlinear Systems*. Wiley-VCH Verlag GmbH, 2008.
8. M. Peeters, R. Viguié, G. Sérandour, G. Kerschen, and J. C. Golinval. Nonlinear normal modes, part II: Toward a practical computation using numerical continuation techniques. *Mechanical Systems and Signal Processing*, 23(1):195–216, 2009.
9. R. Arquier, S. Bellizzi, R. Bouc, and B. Cochelin. Two methods for the computation of nonlinear modes of vibrating systems at large amplitudes. *Computers & Structures*, 84(24-25):1565–1576, 2006.
10. G. Kerschen, M. Peeters, J. C. Golinval, and C. Stéphan. Nonlinear modal analysis of a full-scale aircraft. *Journal of Aircraft*, 50(5):1409–1419, 2013.
11. Sergio R. Idelsohn and Alberto Cardona. A reduction method for nonlinear structural dynamic analysis. *Computer Methods in Applied Mechanics and Engineering*, 49(3):253–279, 6 1985.
12. Paolo Tiso. Optimal second order reduction basis selection for nonlinear transient analysis. In *Modal Analysis Topics, Volume 3*, pages 27–39. Springer, 2011.
13. Frits Wenneker and Paolo Tiso. A substructuring method for geometrically nonlinear structures. In *Dynamics of Coupled Structures, Volume 1*. Springer.

14. J.B. Rutzmoser, D.J. Rixen, and P. Tiso. Model order reduction using an adaptive basis for geometrically nonlinear structural dynamics. In *Conference on Noise and Vibration Engineering, Leuven, Belgium, 20-25 September 2014*.